

## Dense Fe cluster-assembled films by energetic cluster deposition

D. L. Peng,<sup>a)</sup> H. Yamada, and T. Hihara

*Department of Materials Science and Engineering, Nagoya Institute of Technology,  
Nagoya 466-8555, Japan*

T. Uchida

*Department of Applied Chemistry, Nagoya Institute of Technology, Nagoya 466-8555, Japan*

K. Sumiyama

*Department of Materials Science and Engineering, Nagoya Institute of Technology,  
Nagoya 466-8555, Japan*

(Received 12 April 2004; accepted 3 August 2004)

High-density Fe cluster-assembled films were produced at room temperature by an energetic cluster deposition. Though cluster-assemblies are usually sooty and porous, the present Fe cluster-assembled films are lustrous and dense, revealing a soft magnetic behavior. Size-monodispersed Fe clusters with the mean cluster size  $d=9$  nm were synthesized using a plasma-gas-condensation technique. Ionized clusters are accelerated electrically and deposited onto the substrate together with neutral clusters from the same cluster source. Packing fraction and saturation magnetic flux density increase rapidly and magnetic coercivity decreases remarkably with increasing acceleration voltage. The Fe cluster-assembled film obtained at the acceleration voltage of  $-20$  kV has a packing fraction of  $0.86\pm 0.03$ , saturation magnetic flux density of  $1.78\pm 0.05$  Wb/m<sup>2</sup>, and coercivity value smaller than 80 A/m. The resistivity at room temperature is ten times larger than that of bulk Fe metal. © 2004 American Institute of Physics. [DOI: 10.1063/1.1801170]

Cluster-assembling<sup>1-3</sup> is a promising alternative to fabricate nanoscale structure-controlled materials with physical and chemical properties, which are significantly different from those of their corresponding bulk counterparts. However, their sooty appearance, low-dense packing, and weak mechanical properties hinder their application. In order to minimize such disadvantages, several groups have proposed bulky nanocrystalline materials and thin films from nanometer size clusters.<sup>1,4-7</sup> Gleiter *et al.* first reported nanocrystalline materials by collection and consolidation of small metallic clusters.<sup>1,4</sup> These materials consist of about 50 vol% crystals and 50 vol% interfaces. Based on an energetic cluster impact (ECI) concept, Haberland *et al.*<sup>5,6</sup> clearly demonstrated the effect of accelerating energy of incident clusters on thin film deposition and its morphology using an alternative sputtering-type cluster source. In this technique, electrically charged clusters are accelerated by an electric field of an order of a kilovolt and directed onto the substrate, forming compact and almost atomically smooth thin films from small charged clusters (1000–3000 atoms per cluster), while losing the initial cluster size due to hard landing. The films thus produced are highly dense, smooth, and strongly adhering. They also reported that high quality TiN compound films can be produced on room temperature substrates by ECI and the impact energy plays a key role in controlling the smoothness of the TiN film surfaces.<sup>7</sup> In this letter, we describe dense Fe cluster-assembled films prepared by ECI at room temperature, in which the initial size of most of Fe clusters in the films is roughly maintained by using large Fe clusters ( $d=9$  nm, about  $3.2\times 10^4$  atoms per cluster) and mixing deposition of charged and neutral clusters.

Fe cluster-assembled films were prepared by using the plasma-gas-condensation (PGC)-type cluster beam deposi-

tion apparatus (Fig. 1), which is based on plasma-glow-discharge vaporization (sputtering) and inert gas condensation techniques.<sup>8</sup> The background pressure of all chambers (sputtering, cluster-forming and depositing chambers) was  $<1.3\times 10^{-5}$  Pa. During cluster deposition, a large amount of 99.9999% purity Ar and 99.99995% purity He gases of  $1.87-4.1\times 10^{-4}$  mol/s ( $1$  mol/s =  $1.34\times 10^6$  sccm) were introduced continuously into the sputtering chamber and evacuated by a mechanical booster pump through a nozzle, making the sputtering chamber pressure approximately  $1-7\times 10^2$  Pa. Fe atoms sputtered into the inert gas space are decelerated by collisions with Ar and He gas atoms and collide with each other to form Fe clusters. Using the PGC cluster beam deposition apparatus, size-monodispersive Fe clusters with mean sizes  $d$  from 7 to 16 nm and standard deviation less than 10% of  $d$  were produced,<sup>9</sup> and the high-density Fe cluster-assembled films were obtained by ECI as described in the following paragraph. Here, it is worth mentioning that, in the cluster size range of  $d=7-16$  nm, only bcc Fe clusters surrounded by a thin oxide shell layer (1–2 nm) were observed by transmission electron microscopy (TEM) due to exposing them to the ambient atmosphere during sample transfer from the cluster source apparatus to the TEM, being the same as observation results for Fe clusters from a very similar source,<sup>10</sup> while metastable crystal structure (such as fcc) and morphology (such as icosahedron) were not detected although it was reported that almost all as-grown Au clusters ( $d=3-14$  nm) from a gas deposition method are in metastable (icosahedral and decahedral) states.<sup>11</sup>

Fe clusters are partially charged and no additional ionization process is necessary for ionizing clusters because they reside in the plasma region where the electron and ion densities are high.<sup>5-7</sup> The large clusters, which are formed in the cluster growth room and cooled by liquid nitrogen, are

<sup>a)</sup>Electronic mail: pengdl@mse.nitech.ac.jp

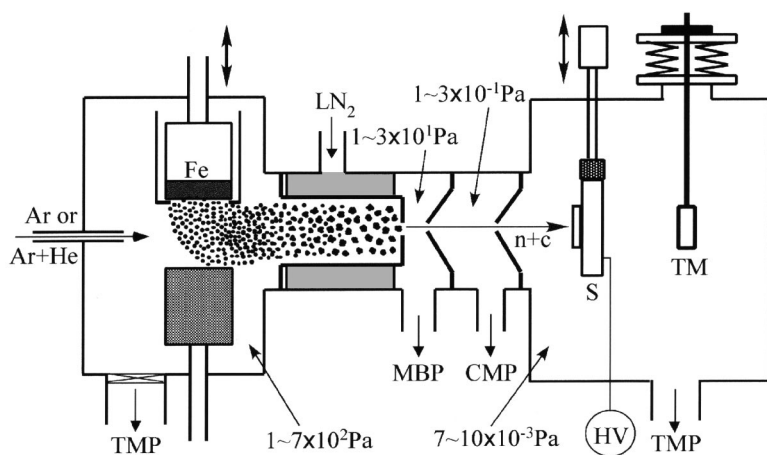


FIG. 1. Schematic drawing of PGC-type cluster deposition apparatus and energetic cluster impact method. TMP, MBP, and CMP represent turbo-molecular pump, mechanical booster pump, and compound molecular pump, respectively. Charged or ionized clusters (c) in cluster beam were accelerated electrically and deposited onto the substrate holder (S) together with neutral clusters (n) from the same cluster source.

ejected from a small nozzle by differential pumping and part of the cluster beam is intercepted by two skimmers, and then deposited onto a metallic sample holder (S) which can be kept at a voltage  $V_a$  up to  $\pm 25$  kV in the deposition chamber ( $7\text{--}10 \times 10^{-3}$  Pa). Based upon deposition experiments of total and charged Fe clusters, we roughly estimated that there are about 20% positively charged clusters, 20% negatively charged clusters, and 60% neutral clusters in our Fe cluster beam. In this experiment, we applied negative  $V_a$  from 0 to  $-20$  kV, and obtained the Fe cluster-assembled films consisting of neutral clusters and positive charged clusters which are accelerated by  $V_a$ . We prepared Fe cluster-assembled films on TEM microgrids for TEM observation, on Si wafers for scanning electron microscopy observation, on polyimide films for magnetic measurement, and on glass substrates for superconducting quantum interference device magnetometer.

Figure 2 shows the plan-view and cross-sectional SEM images of the Fe cluster-assembled films with the initial cluster size  $d=9$  nm at (a) acceleration voltage  $V_a=0$  kV; (b)  $V_a=-20$  kV. For  $V_a=0$  kV [Fig. 2(a)], namely soft-landed Fe clusters, the plan-view image shows very bumpy film surfaces containing inhomogeneous aggregation of Fe clusters and the cross-sectional image reveals a near-random

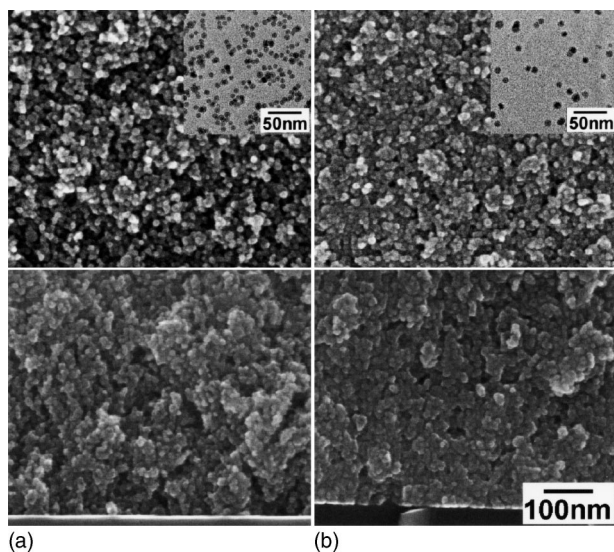


FIG. 2. Plan-view and cross-sectional SEM image of the Fe cluster-assembled films with the initial mean cluster size  $d=9$  nm under (a)  $V_a=0$  and (b)  $-20$  kV. The insets show bright field TEM images of Fe clusters at the initial deposition stages for  $V_a=0$  and  $-20$  kV.

stacking of Fe clusters and a very porous structure which gives a sooty appearance. Moreover, individual Fe clusters are distinguishable. In contrast, the sample obtained with  $V_a=-20$  kV shows a lustrous appearance; both plan-view and cross-sectional images [Fig. 2(b)] clearly reveal a much more high-density cluster-stacking structure than that with  $V_a=0$  kV. Relative to the bulk Fe density, the packing fractions ( $P$ ) (see Table I) of the cluster-assembled films were estimated from the volume and weight of deposition films. We obtained the volumes by measuring the area and thickness of deposited films using SEM and a surface stylus instrument, and the weight by resolving Fe clusters in a hydrochloric acid and chemically analyzing with an atomic absorption spectroscopy. As seen from Table I,  $P$  increases rapidly with increasing  $V_a$ . For  $V_a=0$  kV,  $P$  is only  $0.31 \pm 0.01$  while  $P$  increases up to  $0.86 \pm 0.03$  when  $V_a=-20$  kV, which exceeds the fcc or hcp packing fraction (0.74) in the hard sphere model. For  $V_a=-20$  kV, the impact energy of clusters is estimated to be about  $0.6$  eV/atom for  $d=9$  nm. Since the energy values are one order lower than the cohesive energy of Fe ( $4.47$  eV/atom), it is improbable that all clusters collide with each other to be destroyed completely and recrystallize. In addition, as shown in the insets of Fig. 2, the TEM images of Fe clusters at the initial deposition stages exhibit that there is no marked change in the morphology of the clusters for  $V_a=0$  and  $-20$  kV. Using an image-analysis software (Image-Pro PLUS; Media Cybernetics), we further estimated precisely the size distributions of the clusters (about 400 clusters) not touching and overlapping each other in the digitized images recorded by a slow scan CCD camera in the object area of  $350 \times 350$  nm<sup>2</sup>. The estimated mean cluster sizes are  $d=9.0$  and  $9.7$  nm with standard deviations  $\sigma=0.86$  and  $1.1$  nm for  $V_a=0$  and  $-20$  kV, respectively. Both  $d$  and  $\sigma$  values for  $V_a=-20$  kV are slightly larger than that for  $V_a=0$  kV. These results sug-

TABLE I. Packing fraction, saturation magnetic flux density, and coercivity values of the Fe cluster-assembled films with the initial cluster size  $d=9$  nm under several acceleration voltages.

$V_a$ (kV)	$P$	$B_s$ (Wb/m <sup>2</sup> )	$H_c$ (A/m)	$M_s$ ( $\times 10^{-4}$ Wb m/kg)
0	$0.31 \pm 0.01$	$0.34 \pm 0.01$	$1.37 \times 10^4$	$1.37 \pm 0.02$
-10	$0.52 \pm 0.02$	$0.82 \pm 0.02$	$1.02 \times 10^4$	$1.99 \pm 0.02$
-15	$0.82 \pm 0.02$	$1.59 \pm 0.04$	$2.31 \times 10^2$	$2.45 \pm 0.03$
-20	$0.86 \pm 0.03$	$1.78 \pm 0.05$	$< 7.96 \times 10^1$	$2.70 \pm 0.03$

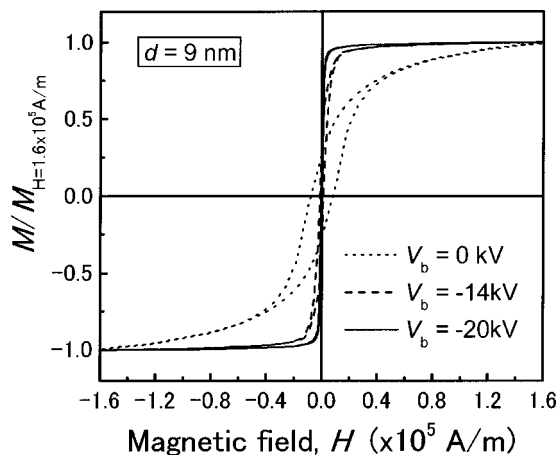


FIG. 3. In-plane hysteresis loops of the Fe cluster-assembled films deposited by ECI with different acceleration voltages. The initial mean cluster size was  $d=9$  nm.

gest that in the present cluster-assembled films by ECI, most of the Fe clusters roughly retain their initial size while part of the Fe clusters was deformed and/or destroyed, leading to formation of Fe cluster-assembled films with a high packing fraction ( $0.86 \pm 0.03$ ) which is larger than the fcc or hcp packing fraction (0.74) in the hard sphere model.

Figure 3 shows the in-plane hysteresis loops of the Fe cluster-assembled films deposited on room temperature substrates by ECI with different  $V_a$  values, where the initial mean cluster size was  $d=9$  nm. The magnetic coercivity,  $H_c$ , dramatically decreases with increasing  $V_a$ . For  $V_a=-20$  kV,  $H_c$  becomes smaller than 80 A/m. Moreover, the magnetization becomes saturated rapidly with increasing  $V_a$ . Therefore, the Fe cluster-assembled films prepared by ECI well reveal a soft magnetic property. We list saturation magnetic flux density  $B_s$  and  $H_c$  in Table I. Clearly,  $B_s$  increases rapidly with increasing  $V_a$ . For  $V_a=-20$  kV,  $B_s$  becomes  $1.78 \pm 0.05$  Wb/m<sup>2</sup> (namely about 83% of  $B_s$  of bulk  $\alpha$ -iron). This result is quite different from the one for metallic nanocrystalline iron (6–7 nm cluster size) obtained by consolidation, where  $B_s$  is only about 60% of the bulk Fe metal.<sup>4</sup>

Such a soft magnetic behavior in the Fe cluster-assembled films can be interpreted qualitatively by Herzer's random anisotropy model (RAM),<sup>12</sup> which basically stands on a single element system. The coercivity derived from the RAM is expressed as follows:

$$H_c = P_c \langle K \rangle / M_s, \quad (1)$$

$$\langle K \rangle = K_c / \sqrt{N} = K_c^4 d^6 / A^3, \quad (2)$$

where  $M_s$  is saturation magnetization,  $K_c$  a local anisotropy constant,  $N$  a grain number in the ferromagnetic exchange volume,  $A$  an exchange stiffness constant, and  $P_c$  a constant factor defined by the crystalline symmetry, orientation, and grain shape: for instance,  $p_c$  is 0.64 for an ensemble of randomly oriented cubic-crystal particles. For the present Fe cluster-assembled films, with increasing packing fraction of clusters or density, it is expected that not only  $M_s$  but also  $N$  are increased in Eqs. (1) and (2). Thus, we can obtain good soft magnetic properties.

Figure 4 shows the electrical resistivity,  $\rho$ , as a function of temperature,  $T$ , for the Fe-cluster-assembled films prepared at  $V_a=0$  and  $-20$  kV. For  $V_a=0$  kV,  $\rho$  has a high value

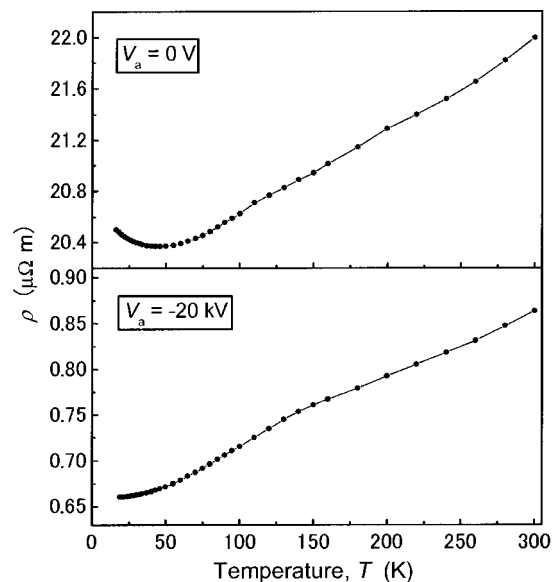


FIG. 4. Electrical resistivity,  $\rho$ , as a function of temperature,  $T$ , for Fe cluster-assembled films with the initial mean cluster size  $d=9$  nm under  $V_a=0$  and  $-20$  kV.

of tens of  $\mu\Omega$  m due to its porous stacking [Fig. 2(a)] and exhibits a minimum at low temperature, being attributable to the weak-localization and/or electron–electron interaction effects in the quasi-two-dimensional network of Fe clusters whose surfaces are partially oxidized due to exposing the sample to the ambient atmosphere.<sup>13</sup> For  $V_a=-20$  kV, the resistivity minimum disappears, and  $\rho$  shows ordinary metallic temperature dependence. Its values are lower than that for  $V_a=0$  kV due to its high cluster-packing fraction. The  $\rho$  value at room temperature is about  $0.86 \mu\Omega$  m. It is an order of magnitude larger than the bulk Fe value owing to conduction electron scattering at cluster–cluster interfaces.

This work has been supported by Grant-in-aid for Intellectual Cluster Project supported by the Ministry of Education, Science, Culture and Sports, Japan, Aichi Prefecture and Aichi Science and Technology Foundation. The authors appreciate K. Takada for his assistance in the atomic absorption spectroscopy measurement.

<sup>1</sup>H. Gleiter, Prog. Mater. Sci. **33**, 223 (1989).

<sup>2</sup>R. Ueda, Prog. Mater. Sci. **35**, 1 (1991).

<sup>3</sup>P. Melinon, V. Paillard, V. Dupuis, A. Perez, P. Jensen, A. Hoareau, M. Broyer, J. L. Vaille, M. Pellarin, B. Baguenard, and J. Lerme, Int. J. Mod. Phys. B **9**, 397 (1995).

<sup>4</sup>R. Birringer, U. Herr, and H. Gleiter, Trans. Jpn. Inst. Met. **27**, 43 (1986).

<sup>5</sup>H. Haberland, M. Karrais, M. Mall, and Y. Thurner, J. Vac. Sci. Technol. A **10**, 3266 (1992).

<sup>6</sup>H. Haberland, M. Mall, M. Moseler, Y. Qiang, T. Reiners, and Y. Thurner, J. Vac. Sci. Technol. A **12**, 2925 (1994).

<sup>7</sup>Y. Qiang, Y. Thurner, T. Reiners, H. Haberland, and O. Rattunde, Surf. Coat. Technol. **100-101**, 27 (1998).

<sup>8</sup>H. Haberland, M. Karrais, and M. Mall, Z. Phys. D: At., Mol. Clusters **20**, 413 (1991).

<sup>9</sup>D. L. Peng, T. Hihara, K. Sumiyama, and H. Morikawa, J. Appl. Phys. **92**, 3075 (2002).

<sup>10</sup>T. Vystavel, G. Palasantzas, S. A. Koch, and J. Th. M. De Hosson, Appl. Phys. Lett. **82**, 197 (2003).

<sup>11</sup>K. Koga, T. Ikeshoji, and K. Sugawara, Phys. Rev. Lett. **92**, 115507 (2004).

<sup>12</sup>G. Herzer, IEEE Trans. Magn. **26**, 1397 (1990).

<sup>13</sup>D. L. Peng, T. Hihara, and K. Sumiyama, Phys. Status Solidi A **196**, 450 (2003).

Applied Physics Letters is copyrighted by the American Institute of Physics (AIP). Redistribution of journal material is subject to the AIP online journal license and/or AIP copyright. For more information, see <http://ojps.aip.org/aplo/aplcr.jsp>  
Copyright of Applied Physics Letters is the property of American Institute of Physics and its content may not be copied or emailed to multiple sites or posted to a listserv without the copyright holder's express written permission. However, users may print, download, or email articles for individual use.